博士学位論文要約（平成 23 年 9 月）

Imaging of Transverse Cross Section of Carotid Artery Using Diverging Transmit Beams from Linear Array Ultrasonic Transducer with Multiple Steered Receive Beamforming

Akinlolu PONNLE
Supervisor: Hiroshi KANAI,　Research Advisor: Hideyuki HASEGAWA

Transverse cross sectional ultrasound imaging of the intima-media complex of the carotid arterial wall is very difficult using conventional linear scanning. The extent of the arterial wall that is clearly imaged is very limited. The use of multi-element diverging beam from a linear array transducer with parallel steered receive beamforming and scanning in a linear sequential fashion is proposed. The B-mode image is reconstructed from combinations of many steered receiving beams from multiple transmissions per frame. In order to further suppress receive grating lobe artifacts in re-constructed B-mode images, a technique is proposed, which involves modulating the receiving beams by a factor that is governed by the envelope of a corresponding signal, formed by filtering the receiving beam by a bidirectional zero phase low-pass filter with a cut-off frequency that is determined by the receive-steering angle.

Using these methods, offline reconstructed B-mode images from simulations, silicone-rubber tube phantom and *in vivo* imaging of the carotid artery showed that the extent of the clearly imaged region is wider than that of conventional linear scanning. Also, receive-grating lobe artifacts were suppressed without significant loss in spatial resolution.

1. Introduction

Ultrasound imaging of the intima-media complex of the carotid arterial wall in the transverse cross-sectional plane is very difficult using conventional linear scanning as the extent of the arterial wall that are clearly imaged is very limited. The intima-media region of the artery is a useful place to probe in the diagnosis of atherosclerosis [1].The *angular width* of the limited imaged region is a measure of the extent of the anterior and posterior walls of the arterial cross-section that are clearly imaged, if the transverse cross-section of the arterial lumen is assumed to be circular.

The use of multi-element diverging beam from a linear array transducer with parallel steered receive beamforming and scanning in a linear sequential fashion is proposed in order to obtain a wider angular width of imaged region without steering of transmit beams and at the same frame rate as in conventional linear scanning. This type of beam has previously been investigated by some researchers for diverse purposes [2,3]. B-mode image was reconstructed from combinations of many steered receiving beams from multiple transmissions per frame. The transmission and reception scheme of the proposed method is illustrated in Fig. 1.

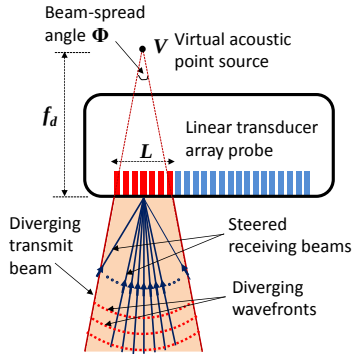

Figure 1 Illustration of the transmission-reception scheme of the proposed method.

In Fig. 1, f_d is the distance from the virtual acoustic point source to the array surface, and L is the transmit sub-aperture length.

Since the transmitted beams are wide, strong reception is possible from the directions of the receive-main lobe and receive-grating lobes leading to grating lobe artifacts. Therefore, a method of modulating the receiving beams was proposed to further suppress grating lobe artifacts.

2. Principle

The principle of the proposed imaging method using multi element diverging transmit beams is summarized in Fig. 2. In this method, within a transmit-receive event, diverging beams are transmitted from a linear array transducer and echoes are received. From the echoes received, steered receiving beams $\mathbf{y}(t,\theta)$ are created offline at regular angular intervals (θ is the receive steering angle). The created, steered receiving beams are then modulated by modulating weights $\mathbf{W}(t,\theta)$ before being spatially combined for image formation.

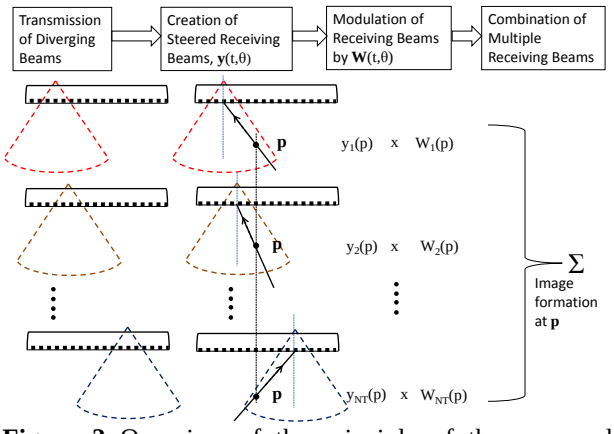

Figure 2 Overview of the principle of the proposed imaging method.

In multi-element diverging beam production, the excitation of each of the elements that make up the transmit sub-aperture is time-delayed so that spherical resultant wavefronts are produced in front of the transducer array over a limited angle. During scanning, coincident active transmit/receive sub-apertures are stepped across the array at a pitch of one element.

For one transmit beam from a transmit sub-aperture, several steered receiving beams in parallel are formed. The maximum steering angle of receiving beams in each transmit beam is limited to ±65 degrees. Angular separation of steered receiving beams is 0.5°. B-mode image was reconstructed from combinations of many steered receiving beams at each image point of interest from multiple transmissions per frame.

Grating lobe artifacts was further suppressed by a technique of modulating the receiving beams by a factor that is governed by the envelope of a corresponding signal, formed by filtering the receiving beam by a bidirectional zero phase Butterworth low-pass IIR filter (ZP-LPF) [4,5], with a cut-off frequency that is determined by the receive-steering angle. The technique is described in Fig. 3.

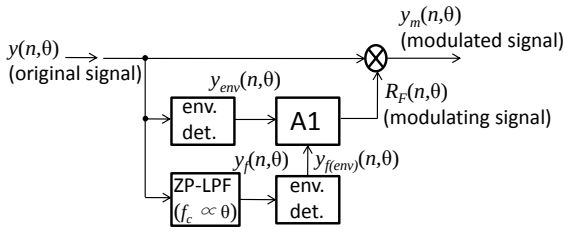

Figure 3 The modulating technique.

The cut-off frequency f_c of the ZP-LPF is expressed as

$$f_c = \frac{c}{p\left(1+\sin|\theta|\right)}, \qquad (1)$$

where c is the speed of ultrasound in the medium, p is the inter-element pitch, and θ is the receive steering angle.

The modulating signal $R_F(n,\theta)$ is obtained by operation A1 defined by

$$R_F(n,\theta) = \begin{cases} \dfrac{y_{f(env)}(n,\theta)}{y_{env}(n,\theta)} & \textbf{if} \quad y_{f(env)}(n,\theta) < y_{env}(n,\theta), \\ 1 & \textbf{otherwise} \end{cases} \qquad (2)$$

where $y_{env}(n,\theta)$ is the envelope of the original receiving beam signal $y(n,\theta)$, and $y_{f(env)}(n,\theta)$ is the envelope of the ZP-LP filtered signal $y_f(n,\theta)$. The output signal $y_m(n,\theta)$ is the modulated receiving beam signal given by

$$y_m(n,\theta) = R_F(n,\theta) \otimes y(n,\theta), \qquad (3)$$

where θ is the receive beam steering angle and (⊗) connotes multiplication.

3. Computer Simulations

3.1 Acoustic Field

The acoustic field of the diverging beam in water from a linear array transducer was simulated using Field II program [6]. Also, the acoustic field in water was measured using a hydrophone (Toray, H025-002), and α-10 ALOKA diagnostic ultrasound equipment with a 10 MHz, 192-element linear array transducer (UST-5545, Aloka Co., Ltd., Tokyo, Japan). Figure 4(1-a) shows the simulated ultrasonic time-pressure waves and Fig. 4(1-b) shows the acoustic pressure as measured by the hydrophone, at a depth of 20 mm below the transducer surface (active transmit sub-aperture of 96 elements and beam-spread angle Φ of 87°). The time axis is referenced to the time of the last element(s) to be fired, which are the two extreme elements in the transmit sub aperture.

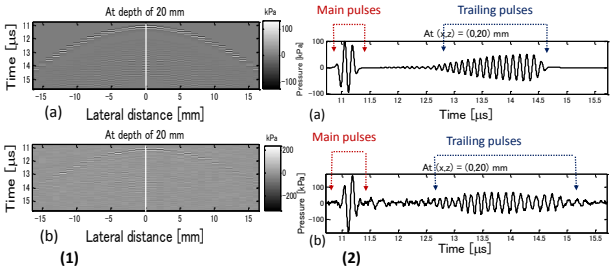

Figure 4(1) (a) Simulated emitted waves and (b) Acoustic pressure as measured with the hydrophone, at axial depth of 20 mm. **4(2)** The emitted pressure waveform as it passes a point below the center of the aperture at an axial depth of 20 mm. (a) Simulation (b) Measurement (waveform along the white lines in (1-a) and (1-b)).

Acoustic field characteristics of the transmit beam from linear array transducer was investigated by simulation using Field II program [6], for beams of various beam-spread angles, Φ ranging from 0° to 180°. The simulated emitted acoustic waveform was found to be a composite of two components which in this research are referred to as 'main pulses' and the 'trailing pulses' (Figs. 4(2-a) and 4(2-b)).

The main pulses are effective for imaging, but the trailing pulses affect the image contrast and cause depth sidelobe and range ambiguity artifacts in B-mode images. The trailing pulses depend on the beam parameters such as the aperture length, inter-element pitch and the beam-spread angle. As the beam-spread angle increases, the absolute amplitude of the main pulses reduces while those of the trailing pulses increases. The spatial and temporal length, as well as the amplitude of the main and trailing pulses, vary for different locations within the beam, but is prominent within the region defined by the boundaries of the two edges of the transmit sub aperture (Fig. 5).

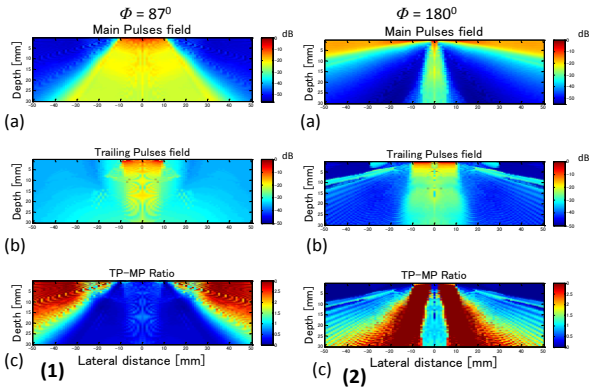

Figure 5 Simulated acoustic fields (from transmit sub aperture of 96 elements), separated into fields due to (a) the main pulses, (b) the trailing pulses and (c) ratio of

the maximum amplitude of the main pulses to the maximum amplitude of the trailing pulses at every point for **(1)** Φ of 87°, and **(2)** Φ of 180°. Similar figures obtain for sub aperture sizes of 56 and 36 elements.

Simulation also shows that within this region, the spatial average ratio of the maximum amplitude of the trailing pulses to the maximum amplitude of the main pulses is less than one (1) for beam-spread angles up to 120° (Fig.6).

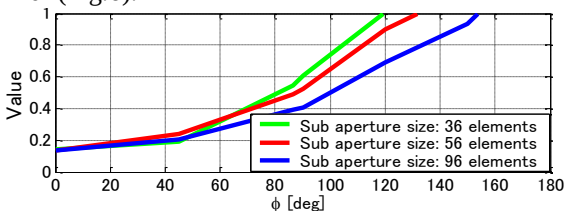

Figure 6 Average ratio of the amplitude of the trailing pulses to main pulses of the acoustic beam between depth of 10 mm and 20 mm below the transducer surface for sub aperture sizes of 36, 56 and 96 elements.

3.2 Virtual Scanning

A 2-interface cylindrical tube composed of point scatterers of inter-scatterer distance of 20 μm (outer wall diameter of 10 mm and inner wall diameter of 8 mm) was simulated, and virtual scanning in the transverse plane, using conventional linear scanning and the proposed scheme with a 192-element linear array transducer, were performed for various beam-spread angles and sub apertures sizes of 36, 56 and 96 elements using Field II program [5]. The center of the tube's cross section is positioned at a depth of 14.1 mm.

Number of transmissions, N_T, for each sub-aperture size is given by

$$N_T = N_{ea} - N_{es} + 1, \qquad (4)$$

where N_{ea} is the number of elements in the array and N_{es} is the number of elements in the sub aperture.

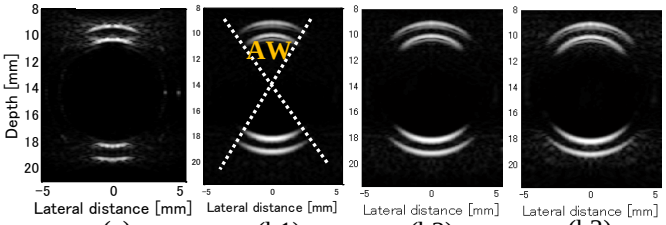

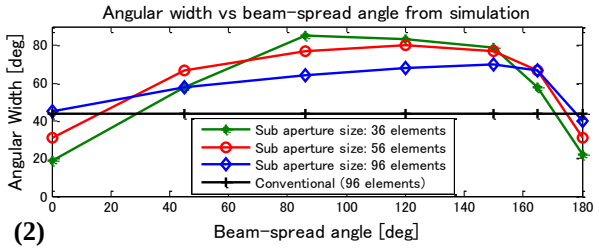

Figure 7(1) B-mode images of the simulated cylindrical tube. (a) Conventional scanning, (b) Diverging beam scanning, beam-spread angle Φ of 87° and sub aperture size of (b1) 96, (b2) 56, and (b3) 36 elements. **7(2)** Variation of angular width (AW) of the imaged region for different Φ and sub aperture sizes of 36, 56 and 96 elements.

Maximum observable angular width of 85° with beam-spread angle of 87° and transmit sub aperture size of 36 elements was obtained from simulations (Fig. 7(2)).

4. Phantom Experiments

A silicone-rubber tube phantom in water was scanned in transverse cross sectional plane using conventional linear scanning and the proposed method for beams with beam-spread angles ranging from 87° to 150°; and sub apertures sizes of 36, 56 and 96 elements. The scanning was performed using α-10 ALOKA ultrasound equipment and a 10 MHz, 192-element linear array transducer probe (UST-5545, Aloka Co., Ltd., Tokyo, Japan). Received ultrasonic RF echoes were sampled at a frequency of 40 MHz. Number of transmissions for each sub-aperture size is given by equation (4).

Figure 8(1) shows the reconstructed B-mode images of the silicone-rubber tube phantom. The plot in Fig. 8(2) shows the variation of the angular width (AW) of the clearly imaged region with different beam-spread angles, Φ, for the silicon-rubber tube phantom in comparison with the angular width obtained with conventional scanning. Maximum angular width of 60° with beam-spread angle of 87° and transmit sub aperture size of 36 elements was obtained from diverging beam scanning as opposed to 24° obtained from conventional linear scanning. This is an increase of about 2.5.

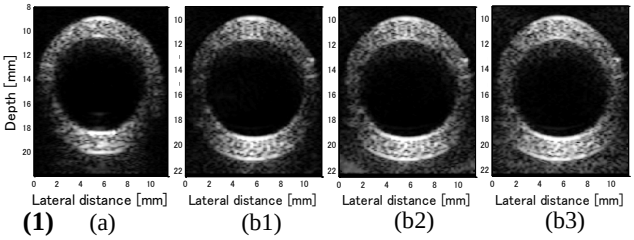

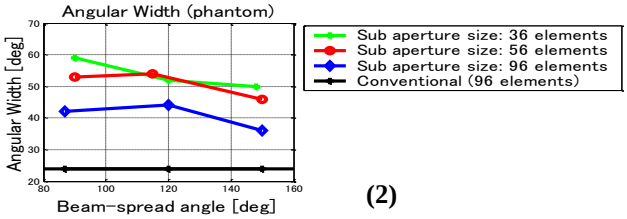

Figure 8(1) B-mode images of the silicone-rubber tube phantom. (a) Conventional scanning. (b) Diverging beam scanning (b1) Φ of 87° and sub aperture of 96 elements, (b2) Φ of 90° and sub aperture of 56 elements, (b3) Φ of 90° and sub aperture of 36 elements. **8(2)** Variation of angular width (AW) of the clearly imaged region for different Φ, and coincident transmit/receive sub-aperture sizes of 36, 56 and 96 elements.

5. *In vivo* Imaging

A beam-spread angle of 90° with transmit sub aperture size of 36 elements were selected for *in vivo* imaging. *In vivo* imaging of the transverse cross section of the carotid artery of three human subjects (adult males) were taken using the α-10 ALOKA ultrasound equipment and the 192-element linear transducer array probe used in the phantom experiments. Two scans were performed in each experiment; conventional

focused linear scanning and the proposed method (diverging beam scanning). Received RF signals were sampled at a frequency of 40 MHz and the elements' received RF data for each transmission were acquired for offline processing.

Figures 9(a) and 9(b) shows the re-constructed B-mode images obtained from the carotid artery scanning of the first subject. Figure 9(b) was re-constructed from 141 sequential transmissions (symmetrical about center of lumen) per frame. Wider regions of the posterior intima and adventitia can be seen in the diverging beam image than in the conventional focused beam image. The average result obtained (from the three subjects) for the angular width from diverging beam scanning is about 45° and 24° from conventional linear scanning; yielding a ratio of about 1.9.

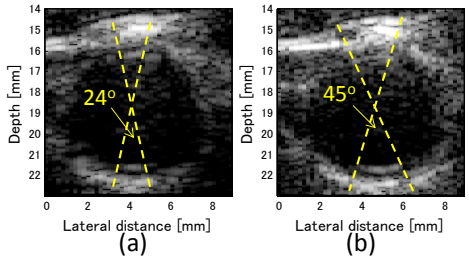

Figure 9 B-mode images of the carotid artery of the first subject in the transverse cross sectional plane. (a) Conventional scanning, (b) Diverging beam scanning, Φ of 90° and transmit/receive sub-aperture size of 36/96 elements. Images are in 50 dB range.

6. Suppression of Grating Lobe Artifacts

The proposed method of suppression of grating lobe artifacts by modulation of receiving beams was applied to reconstructed B-mode image obtained from virtual scanning of simulated columns of point scatterers in water (Fig. 10(1)), and a grating lobe artifact suppression of about 40 dB was realized (Fig. 10(2)).

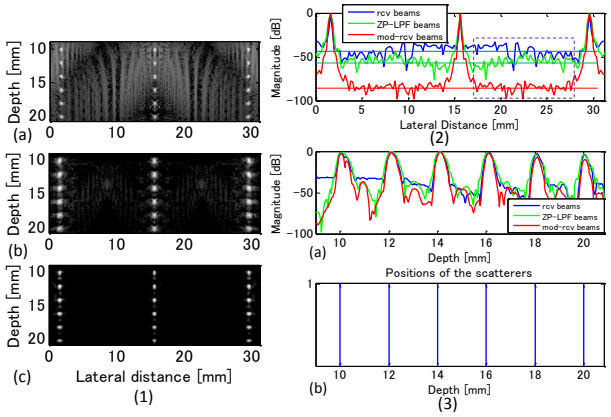

Figure 10(1) Reconstructed B-mode image of virtual scanning of simulated columns of point scatterers using diverging beam scanning, (a) from receiving beams, (b) from ZP-LPF signals and (c) from modulated receiving beams. **10(2)** Lateral profile at a depth of 14 mm. **10(3-a)** Depth profile along the scatterers of the central column, **10(3-b)** Positions of the point scatterers of 10(3-a).

The proposed method of modulation of receiving beams was also applied to the phantom B-mode image, and the *in vivo* images. It suppresses grating lobe artifacts without loss in spatial resolution (Figs. 11(1) and 11(2)).

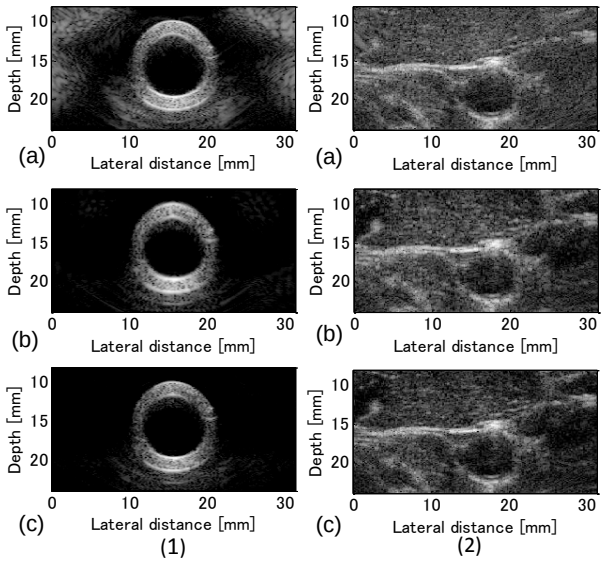

Figure 11 Reconstructed B-mode images of **(1)** silicone-rubber tube phantom in the transverse cross-sectional plane, and **(2)** carotid artery of the first subject in the transverse cross sectional plane (a) from receiving beams, (b) from ZP-LPF signals and (c) from modulated receiving beams. All images are in 60 dB range.

7. Conclusion

This research has demonstrated through simulations, phantom and *in vivo* imaging that by employing multi-element diverging beams from a linear array transducer, improved image of the carotid artery in the transverse cross-sectional plane can be obtained than is possible with conventional linear scanning. In this method, there is no need for steering of transmit beams.

Also, the proposed method of modulation of receiving beams further suppresses receive-grating lobe artifacts. It is effective for keeping the phases of the steered receiving beams unaffected as well for preserving the spatial resolution of the reconstructed image.

References

1) H. Hasegawa and H. Kanai, IEEE Trans. UFFC, **55** (2008) 1921-1934.
2) M. Karaman, P. Li, and M. O'Donnell, IEEE Trans. UFFC, **42** (1995) 429-442.
3) G. R. Lockwood, J. R. Talman, and S. S. Brunke, IEEE Trans. UFFC, **45** (1998) 980-988.
4) F. Gustafsson, IEEE Trans. Signal Process, **44** (1996) 988-992.
5) I. W. Selesnick and C. S. Burrus, Proc IEEE Inter Conf Acoust Speech Signal Proces, **3** (1996) 1688-1694.
6) J. A. Jensen, Med. Biol. Eng. Comp., **34**, (1996) 351-353.